Journal of NUCLEAR SCIENCE and TECHNOLOGY, Supplement 4, p. 283–286 (March 2004)

Development of a New Reconstruction Algorithm for Compton Scattering Imaging

Tran Kim TUAN*, Sung Ho PARK, Jong Kyung KIM

Hanyang University, 17 Haengdang, Sungdong, Seoul 133-791, Korea

A new method for inspection of luggage samples has been investigated by using a 90° Compton scattering system. The algorithm of the system based on measurements of single scattered gamma rays was developed to reconstruct the same physical images of the objects. The algorithm was constructed to estimate the electron density and linear attenuation coefficients by using the responses of scattering detectors and the transmission detector. The over-estimated and under-estimated problem in the calculations of total and Compton attenuation coefficients can be overcome by using iteration method and by introducing adjustment factor with the response of the transmission detector. The images obtained from Monte Carlo simulations using MCNP4C for some common materials were close to the simulated objects. The excellent agreement between calculated values of electron densities and attenuation coefficients in the simulation and actual ones demonstrates the viability of the new reconstruction algorithm as a method for investigating objects.

KEY WORDS: Compton scattering, gamma imaging, electron density, attenuation coefficient

I. Introduction

The Compton scattering of gamma beams has been considered for medical and industrial imaging or luggage inspection for many years based on its advantages in comparison with the transmission tomography. The main attraction of Compton scattering imaging system is that this system can produce directly the electron density images of the object. Compton scattering gives the probability for inspecting objects without having access to two opposing sides of the objects. In this study, a new reconstruction algorithm model of a 90° Compton scattering system for inspection of luggage samples is introduced. The 90° Compton scattering model has a simple reconstruction algorithm because of main advantages: good definition of voxel positions and reduction of Rayleigh scattering effect.

A schematic of the proposed Compton scattering imaging system is shown in **Fig.1**. Considering a mono-energy beam of photons of energy E_0, a photon collides with a free electron and is scattered at an angle θ with respect to its original direction. The energy E of the scattered photon is uniquely related to that of the primary one E_0 and the scattering angle θ by

$$E = \frac{E_0}{1 + \frac{E_0}{m_0 c^2}\left(1 - \cos\theta\right)} \qquad (1)$$

where m_0c^2 (= 0.511 MeV) is the rest mass energy of the electron.

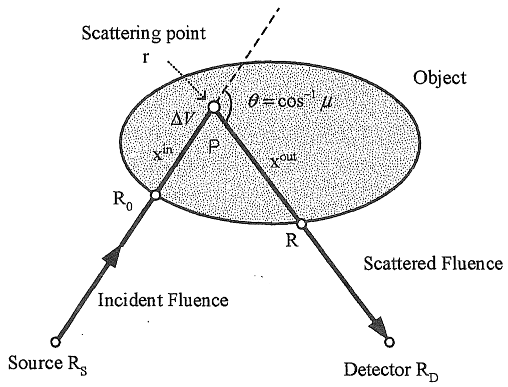

Fig.1 The schematic representation of gamma ray scattering

By shielding both the source and the detectors well and using the unique relation between the scattering angle and the scattering energy in Eq. (1), the scattering detector response may be assumed to result from the single scattered photons. The scattering detector response for a point source and a point detector can be expressed as follows [1]

$$\Psi_S\left(E_0, E\right) = S_0 \frac{k\left(E\right)}{\left|R - r\right|^2} f_i\left(R_0 - r, E_0\right) \Delta V P\left(E_0, E\right) f_S\left(R - r, E\right) \qquad (2)$$

where S_0 is the source intensity, $k(E)$ is the detector efficiency, f_i and f_S are the attenuation factors for the incoming (incident) and outgoing (scattered) pathways respectively, $P(E_0,E)$ is the Compton scattering probability per unit area per electron. The probability $P(E_0,E)$ depends on the electron density $\rho_e(r)$ and can be expressed as $P(E_0,E) = \rho_e(r)\sigma_S(E_0)$. The scattering cross section $\sigma_S(E_0)$ can be determined from the well-known Klein–Nishina scattering differential equation.

* Corresponding author, Tel. +82-2-2299 1732, Fax. +82-2-2294 4800, email: tran@nural.hanyang.ac.kr

The attenuation factors can be expressed as

$$f_i = \exp\left\{-\int_{R_0}^{r} \mu_t\left(E_0, l\right) dl\right\}, \tag{3}$$

$$f_S = \exp\left\{-\int_{r}^{R} \mu_t\left(E, l\right) dl\right\} \tag{4}$$

where $\mu_t(E)$ is the total linear attenuation coefficient of photons along the considered radiation path. The attenuation coefficients are considered as unknowns, hence there are three unknowns in Eq. (2). At high energy of incident gamma rays, the contribution of the photoelectric effect to photon attenuation is small compared to that of Compton scattering. For low atomic-number materials, encountered in the human body and some hydro-carbon industrial materials, it is also reasonable to neglect the photoelectric effects. For solving Eq. (2) with two unknowns remaining, a Compton 90° geometry scattering system is employed as shown in the next section.

II. Compton scattering imaging model

The 90° Compton scattering system as shown in **Fig.2** has some advantages related to the simple imaging reconstruction algorithm. When a beam of gamma rays is incident on the object, the intensities of the transmission and scattering radiation on the angle of 90° are measured at the same time by a transmission detector and 4 scattering detector arrays which are indicated conveniently as top, bottom, left and right.

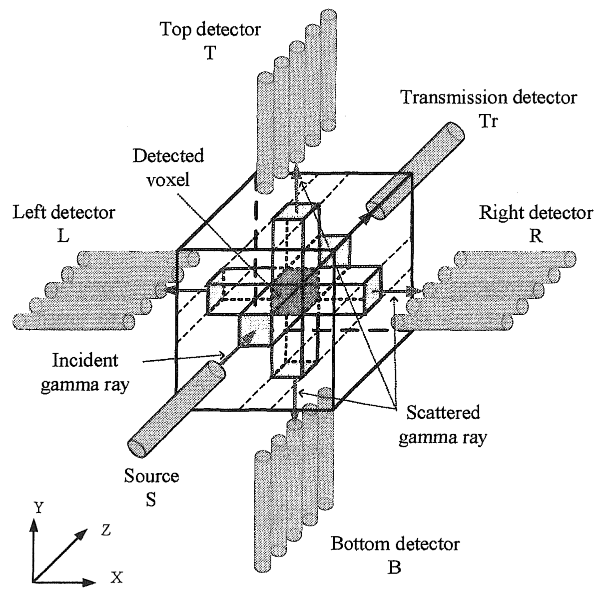

Fig.2 Geometry of 90° Compton scattering system

The incident beam is moved in a plane parallel with the cross section of the object, from left to right and from top to bottom with steps equal the size of a voxel until the entire object is exposed. By this way of exposure, the object can be considered as dividing into NX×NY×NZ voxels, where NX, NY, and NZ are the number of voxels following the direction X, Y, and Z, respectively. To obtain the equation of a scattering detector response, let consider a right scattering detector in the X-Z plane. For simplification, the attenuation effects of gamma rays in the air before a gamma ray comes into the object and after the gamma ray goes out from the object to the detector are neglected. Assuming that the photon is scattered at the center of the voxel, $f_i(\theta,E)$ and $f_S(\theta,E')$ can be obtained by

$$f_i = \exp\left\{-\Delta x^{in} \sum_{m=1}^{k-1} \mu_{i,j,m} - \frac{1}{2}\Delta x^{in} \mu_{i,j,k}\right\}, \tag{5}$$

$$f_S = \exp\left\{-\Delta x^{out} \sum_{m=1}^{i-1} \mu'_{m,j,k} - \frac{1}{2}\Delta x^{out} \mu'_{i,j,k}\right\} \tag{6}$$

if Δx^{in} and Δx^{out} are chosen the same for every voxel in the direction of the incident and scattering pathway, respectively. The detector response can be obtained by substituting Eq. (5) and Eq. (6) to Eq. (2) leading to

$$R_{i,j,k} = R^0_{i,j,k} \mu^C_{i,j,k} \exp\left\{-\Delta x^{in} \sum_{m=1}^{k-1} \mu_{i,j,m} - \frac{1}{2}\Delta x^{in} \mu_{i,j,k} - \Delta x^{out} \sum_{m=1}^{i-1} \mu'_{m,j,k} - \frac{1}{2}\Delta x^{out} \mu'_{i,j,k}\right\} \tag{7}$$

where R and R^0 are the right detector response with/without the objects. Similar expressions can be written for the responses of left, top and bottom scattering detectors. For the transmission detector, one obtains

$$Tr_{i,j} = Tr^0_{i,j} \exp\left(-\Delta x^{in} \sum_{m=1}^{NZ} \mu_{i,j,m}\right) \tag{8}$$

In Eq. (8) there is no indicator k because the incident beam goes through all voxels which lies on the line from the source to the transmission detector. Therefore for exposing whole the object, 4×NX×NY×NZ measurements from the scattering detectors and NX×NY ones from the transmission detector are determined.

1. Reconstruction algorithm for total attenuation coefficient at scattering energy

It is easy to recognize from Eq. (7) that all expressions of scattering detector responses for a voxel consist of the same term of the incoming attenuation factor $f_i(\theta,E)$ and the Compton attenuation μ^C. Therefore a ratio of two scattering detector responses depends on the attenuation coefficient μ' only and μ' can be determined from this ratio. Let consider the first quarter of an object slice that is perpendicular to the incident beam as shown in **Fig.3**.

We rewrite the responses for the voxel (i+1,j,k) as follows

$$B_{i+1,j,k} = d_{i+1,j,k} \exp\left\{-\sum_{m=1}^{j-1} \mu'_{i+1,m,k} \Delta y - \right.$$

$$-\frac{1}{2}\mu'_{i+1,j,k}\Delta y\Big\} \tag{9}$$

$$L_{i+1,j,k} = d_{i+1,j,k}\exp\Big\{-\sum_{m=1}^{i-1}\mu'_{m,j,k}\Delta x - \mu'_{i,j,k}\Delta x - \frac{1}{2}\mu'_{i+1,j,k}\Delta x\Big\} \tag{10}$$

where $d_{i+1,j,k} = C\mu^C_{i+1,j,k}\exp\Big\{-\sum_{m=1}^{k-1}\mu_{i,j,m}\Delta z - \frac{1}{2}\mu_{i,j,k}\Delta z\Big\}$ (11)

C is the system constant. For simplifying, we can choose $\Delta x=\Delta y=\Delta z=\Delta$. Dividing Eq. (9) by Eq. (10), μ' can be obtained by

$$\mu'_{i,j,k} = \frac{1}{\Delta}\Big\{\ln\frac{B_{i+1,j,k}}{L_{i+1,j,k}} + \Delta\sum_{m=1}^{j-1}\mu'_{i+1,m,k} - \Delta\sum_{m=1}^{i-1}\mu'_{m,j,k}\Big\} \tag{12}$$

Using this equation, μ' of the voxels in the cross section can be calculated from left to right in each row for whole first quarter. The calculations of μ' for all possible slices in this manner will give the 3-D image of the object.

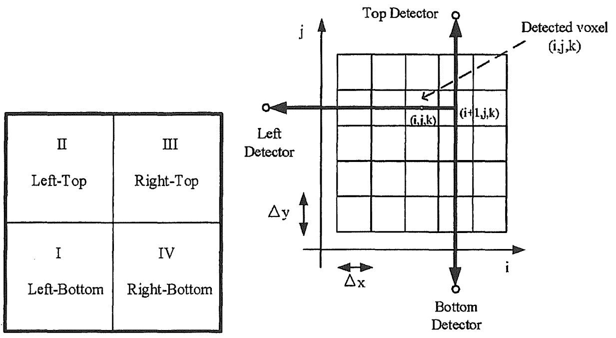

Fig.3 An object slice is considered in 4 quarters with two corresponding scattering detector responses for determining the total attenuation coefficient at the scattering energy. The example using Left and Bottom detector for the first quarter is used to illustrate the calculation method.

2. Reconstruction algorithm for total and Compton attenuation coefficients at incident energy

There are two different methods called by Forward algorithm and Backward algorithm to calculate Compton attenuation coefficient μ^C. Both algorithms can be used and give results in very small difference.

1. Forward Algorithm

In order to calculate μ^C at the incident energy of gamma rays, we can choose the response of any scattering detector. Without lost of generality, bottom detector is chosen here to describe how μ^C can be determined. Rearranging Eq. (9) so that all attenuation coefficients of the voxel (i,j,k) are on the one side of the equation would yield:

$$\mu^C_{i,j,k}\exp\Big(-\frac{1}{2}\mu_{i,j,k}\Delta z\Big) = \frac{B_{i,j,k}}{C}x$$
$$x\exp\Big\{\sum_{m=1}^{k-1}\mu_{i,j,m}\Delta z + \sum_{m=1}^{j-1}\mu'_{i,m,k}\Delta y + \frac{1}{2}\mu'_{i,j,k}\Delta y\Big\} \tag{13}$$

In the gamma energy range from ~100keV to ~1MeV, Compton scattering dominates, the photoelectric absorption is very small compared with the Compton scattering. Hence in this gamma energy range, the Compton cross section being close to the total cross section, it is possible to assume $\mu \approx \mu^C$ then the left term of Eq. (13) depends on μ^C only. Since the right term is known from the previous calculations, Eq. (13) is an equation of μ^C and it can be solved by using any numerical method. The calculation is proceed at first for the voxel nearest the source without μ^C in the right term of Eq. (13), then for the next voxels, so it is called Forward algorithm. Proceeding in this manner, μ^C can be calculated for all voxels of the object.

2. Backward Algorithm

In the different way with the Forward algorithm, two detector responses are used in Backward algorithm: one is a scattering detector and the other is the transmission detector. In the next description, the bottom detector is chosen to illustrate this algorithm. After dividing $B_{i,j,k}$ by $Tr_{i,j,k}$ and rearranging so that all the attenuation coefficients of the voxel (i,j,k) are in one side of the equation, also as in the Forward algorithm, assuming $\mu \approx \mu^C$, one can obtain:

$$\mu^C_{i,j,k}\exp\Big(\frac{1}{2}\mu^C_{i,j,k}\Delta z\Big) = \frac{B_{i,j,k}}{Tr_{i,j,k}}\frac{b}{C}x$$
$$\exp\Big\{-\sum_{m=i+1}^{NZ}\mu^C_{i,j,m}\Delta z + \sum_{m=1}^{j-1}\mu'_{i,m,k}\Delta y + \frac{1}{2}\mu'_{i,j,k}\Delta y\Big\} \tag{14}$$

where b is a system coefficient for the transmission detector. Since the right term can be known from previous calculations, Eq. (14) is an equation for μ^C only and it can be solved. The calculation proceeds at first for the voxel which is farthest from the source, therefore this algorithm is named as Backward algorithm.

Knowing μ^C from Eq. (13) or Eq. (14), μ can be calculated by using the expression of any scattering detector response. It is possible in the gamma energy range where Compton scattering dominates, but the assumption maybe causes that μ^C is over-estimated and μ is under-estimated in comparison with the true value. For more accuracy in estimation of these coefficients, an adjustment using the transmission detector response is introduced and an iteration calculation can be applied. From Eq. (8), one can obtain after a simple arrangement:

$$\sum_{m=1}^{NZ} \mu_{i,j,m} = -\frac{1}{\Delta z} \ln \frac{Tr_{i,j}}{b} \tag{15}$$

The summation of the total attenuation coefficient in the left of this equation is thus available from the transmission measurement and from the $\mu_{i,j,k}$ that is calculated as above. Since the measurement value is usually much more exact than a calculated one, a correction factor ε is defined by

$$\varepsilon = \sum_{m=1}^{NZ} \mu_{i,j,m}^{meas} \Big/ \sum_{m=1}^{NZ} \mu_{i,j,m}^{cal} \quad \text{or}$$

$$\varepsilon = -\frac{1}{\Delta z} \ln\left(\frac{Tr_{i,j}}{b}\right) \Big/ \sum_{m=1}^{NZ} \mu_{i,j,m}^{cal} \tag{16}$$

Then $\mu_{i,j,k}$ is adjusted by

$$\mu_{i,j,k} = \varepsilon \mu_{i,j,k}^{cal} \tag{17}$$

Because $\mu_{i,j,k}$ is more accurate than μ^{cal}, so an iteration process for calculating μ^C and μ can be used.

III. MCNP Simulation

In order to demonstrate the reconstruction algorithm of the method, a small object is used in MCNP simulation, the outputs of which are detector responses. The object consists of 5x5x5 voxels, each voxel is 1x1x1cm cubic. The voxel located in the center of the object is made by a detected material and the others surrounding are made by a background material. The materials used in the simulation are common materials with density in the range of common luggage from 0.94 g/cm^3 of polyethylene up to 8.5 g/cm^3 of brass. The Monte Carlo simulation for the 90^0 Compton scattering system was performed at the source energy 0.662MeV which is in the energy range that Compton scattering dominates.

The calculated results for three different background materials (air, water and polyethylene) show that all of the calculated ρ_e agree with the actual values with errors below 4.6%. The calculated attenuation coefficients also agree with the actual values, where the error is in the range from 0.1% to 5% with the note that the errors are the relative errors compared with the actual values.

IV. Conclusions

A new reconstruction algorithm for the 90° Compton scattering system is developed that is simple compared with other system such as rotating or non-linear system. The results of the MCNP simulation verify that the proposed algorithm can be used to get the image and determine the electron density and attenuation coefficients of the objects with a reasonably good accuracy. The effects of multi-scattering and noise in measurements on quality of images will be considered in the next steps of the work.

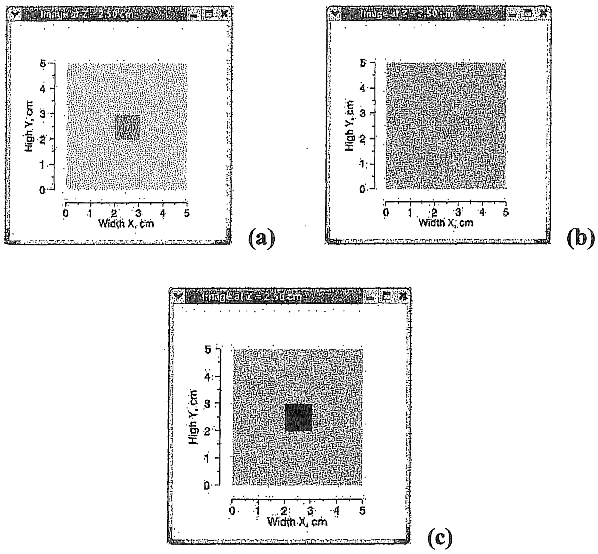

Fig.4 Some object images from MCNP simulation to illustrate the reconstruction algorithm method. **(a)** Image of the object with aluminium detected material and air background in the form of the electron density map. **(b)** Map of total cross sections. The detected material is TNT, the background is polyethylene. **(c)** The image of the object with brass in the centre, and water background in the total cross section map.

Acknowledgement

This work was performed under the long-term nuclear research and development program sponsored by Ministry of Science and Technology of Korea, and sponsored by the Innovative Technology Center for Radiation Safety (iTRS).

References

1) Arendtsz, N.V., Hussein, E.M.A., "Energy-Spectral Compton Scatter Imaging – Part I: Theory and Mathematics," *IEEE Trans. Nucl. Sci,* **42 (6)** 2155-2165 (1995)
2) Arendtsz, N.V., Hussein E.M.A., "Energy-Spectral Compton Scatter Imaging – Part II: Experiments," *IEEE Trans. Nucl. Sci.,* **42 (6)** 2166-1272 (1995)
3) Battista, J.J., Santon, L. W., Bronskill, M.J., "Compton Scatter Imaging of Transverse Sections: Corrections for Multiple Scatter and Attenuations," *Phys. Med. Biol.,* **22 (2)** 229-244 (1977)
4) Cesareo, R., Balogun, F., Brunetti, A., Borlino C.C., "90^O Compton and Rayleigh Measurements and Imaging," *Radiation Phys. Chem.,* **61** 339-342 (2001)
5) Clarke, R.L., Van Dyk, G., "A New Method for Measurement of Bone Mineral Content Using both Transmitted and Scattered Beams of Gamma-rays," *Phys. Med. Biol.,* **18 (4)** 532 (1973)
6) Engler, P., Friedman, W.D. "Review of Dual-Energy Computed Tomography Techniques," Materials Evaluation, **48** 623 (1990)
7) Evans, R.D. "The Atomic Nucleus," Robert E. Krieger Publishing Company, Malabar, Florida, 1982.
8) Kak, A.C. "Principles of Computerized Tomographic Imaging," IEEE Press, New York, 1987.